JACS
JOURNAL OF THE AMERICAN CHEMICAL SOCIETY
COMMUNICATION
pubs.acs.org/JACS

Icosahedral Pt-Centered Pt_{13} and Pt_{19} Carbonyl Clusters Decorated by $[Cd_5(\mu\text{-}Br)_5Br_{5-x}(solvent)_x]^{x+}$ Rings Reminiscent of the Decoration of Au−Fe−CO and Au-Thiolate Nanoclusters: A Unifying Approach to Their Electron Counts

Cristina Femoni, Maria Carmela Iapalucci, Giuliano Longoni, Stefano Zacchini,* and Salvatore Zarra

Dipartimento di Chimica Fisica ed Inorganica, Università di Bologna, viale Risorgimento 4, 40136 Bologna, Italy

Supporting Information

ABSTRACT: The new $[Pt_{13}(CO)_{12}\{Cd_5(\mu\text{-}Br)_5Br_2(dmf)_3\}_2]^{2-}$ and $[Pt_{19}(CO)_{17}\{Cd_5(\mu\text{-}Br)_5Br_3(Me_2CO)_2\}\{Cd_5(\mu\text{-}Br)_5Br(Me_2CO)_4\}]^{2-}$ clusters have been obtained in good yields by reaction of $[Pt_{12}(CO)_{24}]^{2-}$ with $CdBr_2 \cdot H_2O$ in dmf at 90 °C and structurally characterized by X-ray diffraction. Their structures consist of a Pt-centered $Pt_{13}(CO)_{12}$ icosahedron and a $Pt_{19}(CO)_{17}$ interpenetrated double icosahedron, respectively, decorated by two $Cd_5(\mu\text{-}Br)_5Br_{5-x}(solvent)_x$ rings. Their surface decoration may be related to that of Au−Fe−CO clusters as well as to the staple motifs stabilizing gold−thiolates nanoclusters. An oversimplified and unifying approach to interpret their electron count is suggested.

Hydrated $CdX_2 \cdot nH_2O$ (X = Cl, Br) halide salts are emerging as very versatile reagents for the synthesis of metal carbonyl clusters since they may behave as both Lewis and Brønsted acids. As Lewis acids they seek electron density at the surface of the metal carbonyl cluster and coordinate *via* Lewis acid−base interactions, e.g. $Pt_3(CO)_3(PPh(i\text{-}Pr)_2)_3(\mu_3\text{-}CdX_2)$,[1] $\{\eta^2\text{-}\mu_6\text{-}Cd_2(\mu\text{-}Cl)_3[Ni_6(CO)_{12}]_2\}^{3-}$[2] and $[Pt_9(CO)_{18}(\mu_3\text{-}CdCl_2)_2]^{2-}$.[3] The presence on opposite sides of two coordinated $\mu_3\text{-}CdCl_2$ moieties triggers the self-assembly of the latter into infinite $\{[Pt_9(CO)_{18}(\mu_3\text{-}CdCl_2)_2]^{2-}\}_\infty$ chains.[3]

On the other side, the acidity of coordinated water of $CdX_2 \cdot nH_2O$ (X = Cl, Br) salts may also enable concomitant mild oxidation of the anionic metal carbonyl cluster. For instance, the reaction of hydrated $CdX_2 \cdot nH_2O$ salts with $[Ni_9C(CO)_{17}]^{2-}$ or $[Ni_{10}C_2(CO)_{16}]^{2-}$ gives rise to their condensation into high-nuclearity clusters coordinating miscellaneous Cd halide moieties. Several polycarbide species such as $[H_{6-n}Ni_{30}C_4(CO)_{34}(\mu_6\text{-}CdCl)_2]^{n-}$ (n = 3−6),[4] $[H_{4-n}Ni_{22}(C_2)_4(CO)_{28}(\mu_7\text{-}CdBr)_2]^{n-}$ (n = 2−4),[5] and $[H_{5-n}Ni_{36}C_8(CO)_{36}(\eta^2\text{-}\mu_6\text{-}Cd_2Cl_3)]^{n-}$ (n = 3−5)[6] have been conveniently prepared and characterized. In all of the above species only a maximum of two Cd halide moieties are coordinated. Herein, we report the synthesis and structures of $[Pt_{13}(CO)_{12}\{Cd_5(\mu Br)_5Br_2(dmf)_3\}_2]^{2-}$ and $[Pt_{19}(CO)_{17}\{Cd_5(\mu\text{-}Br)_5Br_3(Me_2CO)_2\}\{Cd_5(\mu\text{-}Br)_5Br(Me_2CO)_4\}]^{2-}$. The inner Pt cluster of these compounds is decorated by two unprecedented $\eta^5\text{-}\mu_6\text{-}[Cd_5(\mu\text{-}Br)_5Br_{5-x}(solvent)_x]^{x+}$ rings.

Both clusters have been obtained in good yields by reacting $K_2[Pt_{12}(CO)_{24}]$ or $[NR_4]_2[Pt_{12}(CO)_{24}]$ (R=Et, Bu) with $CdBr_2 \cdot H_2O$ in dmf at 90 °C for 24 h under nitrogen (see Supporting Information (SI) for full Experimental Details). The $[Pt_{13}(CO)_{12}\{Cd_5(\mu\text{-}Br)_5Br_2(dmf)_3\}_2]^{2-}$ dianion was precipitated by metathesis with a solution of $[NBu_4]Br$ in water, dried under vacuum, and extracted in dmf. Crystals suitable for X-ray diffraction of $[NBu_4]_2[Pt_{13}(CO)_{12}\{Cd_5(\mu\text{-}Br)_5Br_2(dmf)_3\}_2] \cdot dmf$ were obtained by layering isopropanol over its dmf solution.[7] The brown salt is soluble in thf, acetone, acetonitrile, and dmf. In all solvents, it displays a single carbonyl absorption in the terminal region (e.g., ν_{CO} in dmf at 2011 cm^{-1}).

The related $[Pt_{19}(CO)_{17}\{Cd_5(\mu\text{-}Br)_5Br_{5-x}(dmf)_x\}_2]^{n-}$ has been similarly isolated and crystallized with several tetra-substituted ammonium cations. Because of the poor quality of the crystals and disorder of the terminal ligands coordinated to Cd and cations, only the metal framework could be safely established. However, further metathesis with $[PPh_3Me]Br$ and crystallization of the resulting salt from Me_2CO and isopropyl alcohol afforded crystals of the $[PPh_3Me]_2[Pt_{19}(CO)_{17}\{Cd_5(\mu\text{-}Br)_5Br_3(Me_2CO)_2\}\{Cd_5(\mu\text{-}Br)_5Br(Me_2CO)_4\}] \cdot 2Me_2CO$ salt (ν_{CO} in Me_2CO at 2008 cm^{-1}), which enabled full elucidation of its structure.[8]

Interestingly, preliminary ^1H and ^{13}C NMR studies indicate that the terminal dmf and Me_2CO ligands in the above clusters may be easily exchanged with N-donor molecules such as pyridines and amines. The observed lability of the solvent molecules coordinated to Cd together with the intense and neat IR carbonyl absorption may indicate the title clusters as potential markers for biological applications.[9]

The molecular structure of $[Pt_{13}(CO)_{12}\{Cd_5(\mu\text{-}Br)_5Br_2(dmf)_3\}_2]^{2-}$ is reported in Figure 1. It consists of a Pt-centered $Pt_{13}(CO)_{12}$ icosahedron (Figure 2) sandwiched between two $Cd_5(\mu\text{-}Br)_5Br_2(dmf)_3$ fragments (Figure 3) via face-bridging $Cd-Pt_3$ interactions, so as to preserve an idealized C_5 axis.

The radial Pt−Pt distances [2.6956(4)−2.7181(4) Å; average 2.707 Å] are shorter than the tangential ones [2.7653(6)−2.9121(6) Å; average 2.850 Å]. The experimentally determined elongation of the tangential interactions (5.1%) compares favorably with the predicted value (*ca.* 5%) for a rigid sphere model of a homonuclear centered icosahedron.

Received: December 13, 2010
Published: February 3, 2011

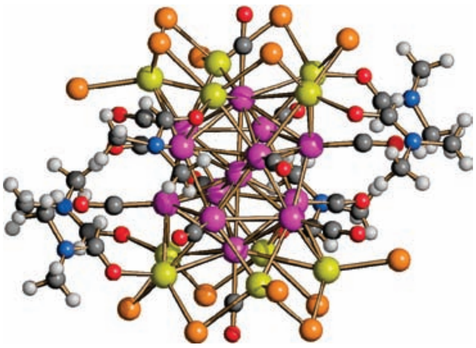

Figure 1. Molecular structure of $[Pt_{13}(CO)_{12}\{Cd_5(\mu\text{-}Br)_5Br_2(dmf)_3\}_2]^{2-}$ (Color scheme: Pt, magenta; Cd, yellow; Br, orange; O, red; C, dark-gray; H, light-gray; N, blue).

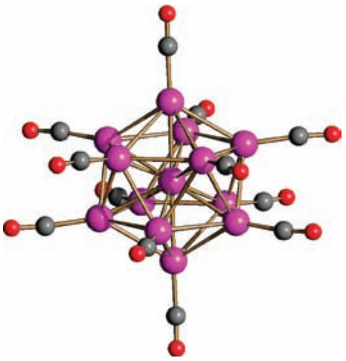

Figure 2. $[Pt_{13}(CO)_{12}]^{8-}$ core of $[Pt_{13}(CO)_{12}\{Cd_5(\mu\text{-}Br)_5Br_2(dmf)_3\}_2]^{2-}$ (Pt−C$_{av}$ 1.84 Å; C−O$_{av}$ 1.14 Å).

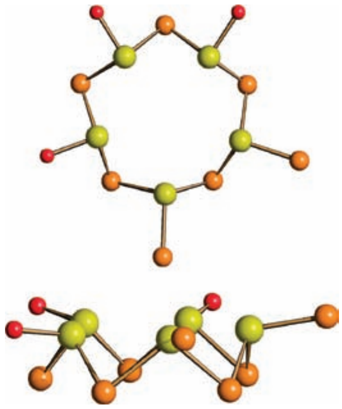

Figure 3. Two views of the $[Cd_5(\mu\text{-}Br)_5Br_2(dmf)_3]^{3+}$ rings (only the O atoms of the coordinated dmf molecules are shown: average Cd−Br$_{br}$ 2.711 Å, Cd−Br$_t$ 2.567 Å, Cd−O 2.231 Å).

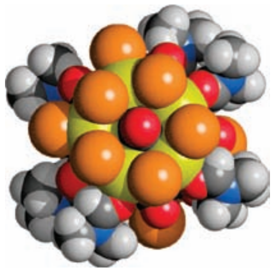

Figure 4. Space filling model of $[Pt_{13}(CO)_{12}\{Cd_5(\mu\text{-}Br)_5Br_2(dmf)_3\}_2]^{2-}$.

Each Cd atom of the ring shows two shorter interactions with two Pt atoms belonging to the Pt_5 ring and one longer interaction with the apical Pt atom. Additionally, the Cd atoms bonded to terminal Br atoms display on average longer Pt−Cd contacts (2.826 and 3.262 Å, respectively) than those coordinated to dmf (2.807 and 3.031 Å, respectively). This, as also pointed out by the space filling model reported in Figure 4, might be a consequence of swelling of the nonbonded Br_5 ring induced by the sub van der Waals contacts between the two apical CO ligands and the bridging bromides. Indeed, the experimental C···Br [3.45−3.67 Å] and, particularly, O···Br [3.48−3.71 Å] contacts are shorter than the sum of van der Waals radii [3.50 and 3.70 Å, respectively].

The electron count of $[Pt_{13}(CO)_{12}\{Cd_5(\mu\text{-}Br)_5Br_2(dmf)_3\}_2]^{2-}$ may be justified by considering separately the Pt carbonyl and Cd halide fragments depicted in Figures 2 and 3. This is followed by evaluation of the decorating Cd halide rings in terms of the Lewis Dot Formula and reassembly of the two rings along one of the C_5 axes of the $Pt_{13}(CO)_{12}$ moiety, *via* either formally ionic or covalent interactions.

In the ionic scheme, an oxidation state of +2 of all Cd atoms is assumed. It follows that the $Cd_5(\mu\text{-}Br)_5Br_2(dmf)_3$ fragment (Figure 3) has an overall charge of +3, with one positive charge formally located on each of the three Cd atoms bearing the dmf ligand. Consideration of electroneutrality leads to the assignment of the Pt_{13} core of $[Pt_{13}(CO)_{12}\{Cd_5(\mu\text{-}Br)_5Br_2(dmf)_3\}_2]^{2-}$ as an octaanion, $[Pt_{13}(CO)_{12}]^{8-}$ (162 CVE).

In the covalent scheme, each $Cd_5(\mu\text{-}Br)_5Br_2(dmf)_3$ moiety is taken as neutral and can contribute 3 electrons (one by each cadmium atom bonded to dmf) by bonding the inner $[Pt_{13}(CO)_{12}]^{2-}$ cluster as a pseudo π-allyl ligand. The latter, therefore, obtains again 162 CVE [13(Pt)×10 + 12(CO) × 2 + 2 + 2(Cd rings)× 3] as above.

Perhaps significantly, both schemes are formally in keeping with the strongest Pt−Cd interactions of the Cd atoms bonded to dmf as a terminal ligand. In any case, according to both of the above alternative descriptions, the inner $Pt_{13}(CO)_{12}$ icosahedral cluster displays 162 CVE, rather than 170 as required by the cluster-borane analogy.[10] The latter number of CVE is adopted by most E-centered Ni and Rh icosahedral carbonyl clusters, such as $[Ni_{12}(\mu_{12}\text{-}E)(CO)_{22}]^{2-}$ (E = Ga, Ge, Sn),[11,12] $[Rh_{12}(\mu_{12}\text{-}Sn)(CO)_{27}]^{4-}$,[13] and $[Rh_{12}(\mu_{12}\text{-}Sb)(CO)_{27}]^{3-}$.[14] Only the recently reported $[Rh_{12}(\mu_{12}\text{-}Sn)(CO)_{26}]^{4-}$ and $[Rh_{12}(\mu_{12}\text{-}Sn)(CO)_{25}]^{4-}$ make exception by featuring 168 and 166 CVE, respectively.[15] Conversely, most gold icosahedral metal clusters (e.g., $[Au_{13}Cl_2(PMe_2Ph)_{10}]^{3+}$[16] and $[Au_9M_4Cl_4(PMe_2Ph)_8]^{+}$ (M = Cu, Ag, and Au)[17,18]) consistently display 162 CVE, as does the above $Pt_{13}(CO)_{12}$. The low electron count of these clusters comprising heavier elements has been explained by Mingos as arising from a predominance of radial over tangential bonding.[19] This conclusion has been recently further supported by DFT calculations on a hypothetical 162 CVE $WAu_{12}(CO)_{12}$ cluster.[20] One other Pt cluster conforming to the above schemes is $Pt_{13}[Au_2(PPh_3)_2]_2(CO)_{10}(PPh_3)_4$[21] in which a formal $[Pt_{13}(CO)_{10}L_4]^{4-}$ core (162 CVE) is decorated by two $[Au_2L_2]^{2+}$ moieties.[22]

The structure of $[Pt_{19}(CO)_{17}\{Cd_5(\mu\text{-}Br)_5Br_3(Me_2CO)_2\}\{Cd_5(\mu\text{-}Br)_5Br(Me_2CO)_4\}]^{2-}$ is shown in Figure 5. Its consists of a $Pt_{19}(CO)_{17}$ interpenetrated double-icosahedron sandwiched along the unique idealized C_5 axis by one $Cd_5(\mu\text{-}Br)_5Br_3(Me_2CO)_2$ ring and one $Cd_5(\mu\text{-}Br)_5Br(Me_2CO)_4$ ring. These are different

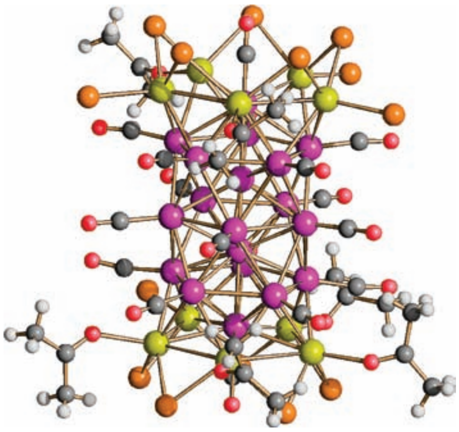

Figure 5. Structure of $[Pt_{19}(CO)_{17}\{Cd_5(\mu\text{-}Br)_5Br_3(Me_2CO)_2\}\{Cd_5(\mu\text{-}Br)_5Br(Me_2CO)_4\}]^{2-}$ (Color scheme: Pt, magenta; Cd, yellow; Br, orange; O, red; C, dark-gray; H, light gray). Average: Pt−C 1.80 Å; C−O 1.17 Å; $Cd-Br_{br}$ 2.741 Å, $Cd-Br_t$ 2.637 Å, Cd−O 2.35 Å.

but closely related to the $Cd_5(\mu\text{-}Br)_5Br_2(dmf)_3$ moieties stabilizing the above $[Pt_{13}(CO)_{12}]^{8-}$ cluster.

The bonding distances in $[Pt_{19}(CO)_{17}\{Cd_5(\mu\text{-}Br)_5Br_3(Me_2CO)_2\}\{Cd_5(\mu\text{-}Br)_5Br(Me_2CO)_4\}]^{2-}$ are very similar to those of $[Pt_{13}(CO)_{12}\{Cd_5(\mu\text{-}Br)_5Br_2(dmf)_3\}_2]^{2-}$. It must be remarked that the shortest Pt−Pt contact is the one between the two central 12-coordinated Pt-atoms [2.5573(16) Å]. Also in this case, the radial Pt−Pt distances [2.5573(16)−2.7933(19) Å; average 2.723 Å] are shorter than the tangential ones [2.7545(19)−2.9761(19) Å; average 2.864 Å] with an elongation of the tangential interactions of 5.0%. Concerning the Pt−Cd contacts, also in this cluster the interactions with the apical Pt atoms [average 3.019 Å] are longer than the ones with the Pt_5 rings [average 2.790 Å].

According to the ionic scheme suggested for $[Pt_{13}(CO)_{12}\{Cd_5(\mu\text{-}Br)_5Br_2(dmf)_3\}_2]^{2-}$, the $Cd_5(\mu\text{-}Br)_5Br_3(Me_2CO)_2$ fragment has an overall charge of +2, with one positive charge formally localized on each of the two Cd atoms bearing the Me_2CO ligand. Conversely, $Cd_5(\mu\text{-}Br)_5Br(Me_2CO)_4$ has an overall charge of +4. Therefore, taking into account electroneutrality leads to the formulation of the interpenetrated double icosahedral core of $[Pt_{19}(CO)_{17}\{Cd_5(\mu\text{-}Br)_5Br_3(Me_2CO)_2\}\{Cd_5(\mu\text{-}Br)_5Br(Me_2CO)_4\}]^{2-}$ as a $[Pt_{19}(CO)_{17}]^{8-}$ octaanion (232 CVE). The interpenetrated double icosahedral core of $[Pt_{19}(CO)_{17}]^{8-}$ is unprecedented in metal carbonyl cluster chemistry. To our knowledge the only related example is $Au_{12}Ag_7(PPhMe_2)_{10}(NO_3)_9$[23] which displays a fuzzy electron count owing to the stereochemistry of nitrates. Therefore, a reasonable number of CVE required by such metal architecture can only be guessed by the available rules for condensed clusters.[24] An interpenetrated double icosahedron of a heavy element such as Pt should require 162 × 2 − 90 = 234 CVE (subtraction of 90 CVE is due to sharing of a Pt_7 pentagonal bipyramid, as inferable from the number of CVE of $[Au_7(PPh_3)_7]^{+}$[25−27]). Such a small discrepancy is more than acceptable. Indeed, both figures are reasonable in view of the fact that the prismatic $[Pt_{19}(CO)_{22}]^{4-}$ displays a higher electron count (238 CVE)[28−30] and exhibits two pairs of cathodic and two pairs of anodic one-electron processes, some of which display features of chemical reversibility.[31] The lower electron count of $[Pt_{19}(CO)_{17}]^{8-}$ (232 CVE) compared to $[Pt_{19}(CO)_{22}]^{4-}$ (238 CVE) is in keeping with the formation of further Pt−Pt contacts passing from a prismatic to an antiprismatic structure.

It is worth noting that the surface decoration of the above Pt clusters is related to that of Au−Fe−CO clusters, e.g. $[Au_{21}Fe_{10}(CO)_{40}]^{5-}$.[32] This latter may be seen as deriving from two $[Au_5\{\mu\text{-}Fe(CO)_4\}_5]^{5-}$ rings sandwiching a $[Au_{11}]^{5+}$ centered pentagonal antiprismatic kernel. The major difference is that here the decorations are the Lewis bases while the $[Au_{11}]^{5+}$ kernel is the Lewis acid. Interestingly, these features and the surface decorations of other Au−Fe−CO clusters, e.g. $[Au_{34}Fe_{14}(CO)_{50}]^{8-}$,[32] are reminiscent of those of the so far characterized gold thiolate nanoclusters, viz. $[Au_{25}(S\text{-}CH_2\text{-}CH_2\text{-}Ph)_{18}]^{-}$,[33] $Au_{38}(S\text{-}CH_2\text{-}CH_2\text{-}Ph)_{24}$,[34] and $Au_{102}(S\text{-}p\text{-}benzoic)_{44}$.[35] Indeed, they all contain *ico* and *poly ico* Au kernels comprising a lower number of Au atoms than indicated by their whole formula (13, 23, 79, respectively), because their kernels are decorated by $[Au(SR)_2]^{-}$ and/or $[Au_2(SR)_3]^{-}$ moieties (so-called *staples*). The electron count of their inner gold kernels can be likewise interpreted by the formal separation of the surface decorations and reassembly *via* the above ionic or covalent schemes. As an example, the Lewis Dot Formula of staples such as $[Au(SR)_2]^{-}$ and $[Au_2(SR)_3]^{-}$ points out that these essentially behave as 4-electron donors analogous to an $R_2P\text{-}(CH_2)_n\text{-}PR_2$ diphos. The major difference is that substitution of the CH_2 moieties with Au(I) or *zigzag* Au(I)-SR-Au(I) backbones triggers intervention of $d^{10}-d^{10}$ Au−Au attractive dispersive interactions.[36] Such an interpretation makes the electron counts of $[Au_{25}(S\text{-}CH_2\text{-}CH_2\text{-}Ph)_{18}]^{-}$,[33] $Au_{38}(S\text{-}CH_2\text{-}CH_2\text{-}Ph)_{24}$,[34] and $Au_{102}(S\text{-}p\text{-}benzoic)_{44}$[35] consistent with those of low-valent organometallic *ico* and *poly ico* clusters of comparable size. For instance, $[Au_{25}(S\text{-}CH_2\text{-}CH_2\text{-}Ph)_{18}]^{-}$, viewed as deriving from stabilization of a $[Au_{13}]^{5+}$ kernel (138 CVE) by decoration with 6 $[Au_2(SR)_3]^{-}$ staples (contributing 6 × 4 = 24 CVE), will become a monoanion and gather 162 CVE as all icosahedral Au clusters cited above or the title $[Pt_{13}(CO)_{12}\{Cd_5Br_7(dmf)_3\}_2]^{2-}$ compound. Likewise, the face-fused bis-icosahedral Au_{23} kernel of $Au_{38}(S\text{-}CH_2\text{-}CH_2\text{-}Ph)_{24}$,[34] once the whole cluster is partitioned as deriving from a $[Au_{23}]^{9+}$ kernel (244 CVE) stabilized and decorated by 3 $[Au(SR)_2]^{-}$ (contributing 3 × 4 = 12 CVE) and 6 $[Au_2(SR)_3]^{-}$ (contributing 6 × 4 = 24 CVE) staples, will become neutral and obtain 280 CVE, as required by a heavy-element face-fused bis-icosahedron (CVE = 162 × 2 − 44 (or 42) = 280 (or 282); subtraction of 44 (or 42) CVE is due to the shared triangular face).[24]

In conclusion, the reported Pt−Cd clusters and their oversimplified bonding analysis according to either an ionic or a covalent scheme suggests an interpretation of the electron count of all pertinent miscellaneous clusters. It turns out that also the electron counts of Au clusters decorated with $[Au_n(SR)_{n+1}]^{-}$ staples are analogous to those of low-valent organometallic clusters.[37] Beyond other considerations, the above schemes provide a rationale for the uniqueness of gold thiolate clusters. Shortly, the thiolate nature of the ligands implies the presence of Au(I), which has a strong preference for digonal coordination. This leads to formation of $[Au_n(SR)_{n+1}]^{-}$ staples, which behave as a 4-electron donor to the kernel and, moreover, enable the insurgence of weak but significant $d^{10}-d^{10}$ dispersive interactions. The above bonding scheme may also be of some help in envisioning more reliable structural models of gold thiolates, once their exact composition is known. Therefore, molecular metal cluster chemistry may give fundamental contributions to the understanding of some facets of nanochemistry and may provide a reliable guideline to interpret ligand-stabilized metal nanoparticles.

ASSOCIATED CONTENT

Ⓢ Supporting Information. CIF files giving X-ray crystallographic data for the structure determination of $[NBu_4]_2[Pt_{13}(CO)_{12}\{Cd_5(\mu\text{-}Br)_5Br_2(dmf)_3\}_2]\cdot dmf$ and $[PPh_3Me]_2[Pt_{19}(CO)_{17}\{Cd_5(\mu\text{-}Br)_5Br_3(Me_2CO)_2\}\{Cd_5(\mu\text{-}Br)_5Br\ (Me_2CO)_4\}]\cdot 2Me_2CO$. Experimental details on the synthesis of $[NBu_4]_2[Pt_{13}(CO)_{12}\{Cd_5(\mu\text{-}Br)_5Br_2(dmf)_3\}_2]\cdot dmf$ and $[PPh_3Me]_2[Pt_{19}(CO)_{17}\{Cd_5(\mu\text{-}Br)_5Br_3(Me_2CO)_2\}\{Cd_5(\mu\text{-}Br)_5Br(Me_2CO)_4\}]\cdot 2Me_2CO$. This material is available free of charge via the Internet at http://pubs.acs.org.

AUTHOR INFORMATION

Corresponding Author

zac@ms.fci.unibo.it

ACKNOWLEDGMENT

We wish to acknowledge the financial support of the University of Bologna and MIUR (PRIN 2008).

REFERENCES

(1) Stockhammer, A.; Dahmen, K.-H.; Gerfin, T.; Venanzi, L. M.; Gramlich, V.; Petter, W. *Helv. Chim. Acta* **1991**, *74*, 989.

(2) Femoni, C.; Iapalucci, M. C.; Longoni, G.; Ranuzzi, F.; Zacchini, S.; Fedi, S.; Zanello, P. *Eur. J. Inorg. Chem.* **2007**, 4064.

(3) Femoni, C.; Kaswalder, F.; Iapalucci, M. C.; Longoni, G.; Zacchini, S. *Chem. Commun.* **2006**, 2135.

(4) (a) Bernardi, A.; Femoni, C.; Iapalucci, M. C.; Longoni, G.; Ranuzzi, F.; Zacchini, S.; Zanello, P.; Fedi, S. *Chem.—Eur. J.* **2008**, *14*, 1924. (b) Bernardi, A.; Femoni, C.; Iapalucci, M. C.; Longoni, G.; Zacchini, S. *Inorg. Chim. Acta* **2009**, *362*, 1239.

(5) Bernardi, A.; Femoni, C.; Iapalucci, M. C.; Longoni, G.; Zacchini, S. *Dalton Trans.* **2009**, 4245.

(6) Bernardi, A.; Femoni, C.; Iapalucci, M. C.; Longoni, G.; Zacchini, S.; Fedi, S.; Zanello, P. *Eur. J. Inorg. Chem.* **2010**, 4831.

(7) Crystal data for $[NBu_4]_2[Pt_{13}(CO)_{12}\{Cd_5(\mu\text{-}Br)_5Br_2(dmf)_3\}_2]\cdot dmf$: $C_{65}H_{121}Br_{14}Cd_{10}N_9O_{19}Pt_{13}$, M=6111.62, T=294(2) K, monoclinic, space group $C2/c$, a = 26.1251(14), b = 15.6936(9), c = 32.851(2) Å, β = 109.2960(10)°, V =12712.3(14) Å^3, Z = 4, D_c = 3.193 g cm^{-3}, μ =20.321 mm^{-1}, graphite-monochromatized Mo Kα radiation (λ = 0.71073 Å). Further details in SI.

(8) Crystal data for $[PPh_3Me]_2[Pt_{19}(CO)_{17}\{Cd_5(\mu\text{-}Br)_5Br_3(Me_2CO)_2\}\{Cd_5(\mu\text{-}Br)_5Br(Me_2CO)_4\}]\cdot 2Me_2CO$: $C_{79}H_{84}Br_{14}Cd_{10}O_{25}P_2Pt_{19}$, M = 7444.85, T = 100(2) K, monoclinic, space group $P2_1/c$, a = 17.2308(19), b = 28.340(3), c = 32.657(4) Å, β = 97.478(2)°, V = 15812(3) Å^3, Z = 4, D_c = 3.127 g cm^{-3}, μ = 21.645 mm^{-1}, graphite-monochromatized Mo Kα radiation (λ = 0.71073 Å). Further details in SI.

(9) Hogarth, G.; Kabir, S. E.; Nordlander, E. *Dalton Trans.* **2010**, *39*, 6153.

(10) (a) Halet, J.-F.; Evans, D. G.; Mingos, D. M. P. *J. Am. Chem. Soc.* **1988**, *110*, 87. (b) Wade, K. *Adv. Inorg. Chem. Radiochem.* **1976**, *18*, 1.

(11) Femoni, C.; Iapalucci, M. C.; Longoni, G.; Zacchini, S. *Eur. J. Inorg. Chem.* **2010**, 1056.

(12) Ceriotti, A.; Demartin, F.; Heaton, B. T.; Ingallina, P.; Longoni, G.; Manassero, M.; Marchionna, M.; Masciocchi, N. *J. Chem. Soc., Chem. Commun.* **1989**, 786.

(13) Femoni, C.; Iapalucci, M. C.; Longoni, G.; Tiozzo, C.; Zacchini, S.; Heaton, B. T.; Iggo, J. A. *Dalton Trans.* **2007**, 3914.

(14) Vidal, J. L.; Troup, J. M. *J. Organomet. Chem.* **1981**, *213*, 351.

(15) Femoni, C.; Iapalucci, M. C.; Longoni, G.; Tiozzo, C.; Zacchini, S.; Heaton, B. T.; Iggo, J. A.; Zanello, P.; Fedi, S.; Garland, M. V.; Li, C. *Dalton Trans.* **2009**, 2217.

(16) Briant, C. E.; Theobald, B. R. C.; White, J. W.; Bell, L. K.; Mingos, D. M. P. *J. Chem. Soc., Chem. Commun.* **1981**, 201.

(17) Copley, R. C. B.; Mingos, D. M. P. *J. Chem. Soc., Dalton Trans.* **1996**, 491.

(18) Copley, R. C. B.; Mingos, D. M. P. *J. Chem. Soc., Dalton Trans.* **1992**, 1755.

(19) Mingos, D. M. P. *J. Chem. Soc., Chem. Commun.* **1985**, 1352.

(20) Johansson, M. P.; Pyykkö, P. *Chem. Commun.* **2010**, *46*, 3756.

(21) de Silva, N.; Dahl, L. F. *Inorg. Chem.* **2005**, *44*, 9604.

(22) The covalent scheme is described in ref 21.

(23) Nunokawa, K.; Ito, M.; Sunahara, T.; Onaja, S.; Ozeki, T.; Chiba, H.; Funahashi, Y.; Masuda, H.; Yonezawa, T.; Nishihara, H.; Nakamoto, M.; Yamamoto, M. *Dalton Trans.* **2005**, 2726.

(24) Mingos, D. M. P.; May, A. S. In *The Chemistry of Metal Cluster Complexes*; Shriver, D. F., Kaesz, H. D., Adams, R. D., Eds.; VCH Publishers: New York, 1990; pp 11−119.

(25) Van der Velden, J. W. A.; Beurskens, P. T.; Bour, J. J.; Bosman, W. P.; Noordik, J. H.; Kolenbrander, N.; Buskes, J. A. K. M. *Inorg. Chem.* **1984**, *23*, 146.

(26) Hall, K. P.; Gilmour, D. J.; Mingos, D. M. P. *J. Organomet. Chem.* **1984**, *268*, 275.

(27) Briant, C. E.; Hall, K. P.; Mingos, D. M. P. *J. Chem. Soc., Chem. Commun.* **1984**, 248.

(28) Washecheck, D. M.; Wucherer, E. J.; Dahl, L. F.; Ceriotti, A.; Longoni, G.; Manassero, M.; Sansoni, M.; Chini, P. *J. Am. Chem. Soc.* **1979**, *101*, 6110.

(29) Application of Topological Electron-Counting Theory to $[Pt_{19}(CO)_{22}]^{4-}$ would predict 244 CVE. Nonetheless, as originally noticed, platinum carbonyl clusters are often under the required electron count.[30] A similar consideration applies to $[Pt_{19}(CO)_{17}]^{8-}$ herein reported.

(30) (a) Teo, B. K. *Inorg. Chem.* **1984**, *23*, 1251. (b) Teo, B. K.; Longoni, G.; Chung, F. R. K. *Inorg. Chem.* **1984**, *23*, 1257.

(31) Fedi, S.; Zanello, P.; Laschi, F.; Ceriotti, A.; El Afefey, S. *J. Solid State Electrochem.* **2009**, *13*, 1497.

(32) Femoni, C.; Iapalucci, M. C.; Longoni, G.; Tiozzo, C.; Zacchini, S. *Angew. Chem., Int. Ed.* **2008**, *137*, 483.

(33) Zhu, M.; Aikens, C. M.; Hollander, F. J.; Schatz, G. C.; Jin, R. *J. Am. Chem. Soc.* **2008**, *130*, 5883.

(34) Qian, H.; Eckenhoff, W. T.; Zhu, Y.; Pintauer, T.; Jin, R. *J. Am. Chem. Soc.* **2010**, *132*, 8280.

(35) Jadzinsky, P. D.; Calero, G.; Ackerson, C. J.; Bushnell, D. A.; Komberg, R. D. *Science* **2007**, *318*, 430.

(36) Jansen, M. *Angew. Chem., Int. Ed. Engl.* **1987**, *26*, 1098.

(37) Longoni, G.; Iapalucci, M. C. In *Clusters and Colloids*; Schmid, G., Ed.; VCH: Weinheim, 1994; pp 91−177.